Journal of Inclusion Phenomena 3, 125–133. 0167–7861/85.15.

Laser Microprobe Mass Analysis (LAMMA) of Pyridine Adsorbed on Some Clay Minerals from Turkey

S. AKYÜZ★
Department of Physics (Fizik-83), Hacettepe University, Beytepe, Ankara, Turkey

J. K. WAELE
Department of Chemistry, University of Antwerp (UIA), B-2610 Wilrijk, Belgium

T. AKYÜZ
Mineral Research and Exploration Institute (MTA), Balgat, Ankara, Turkey

and

F. C. ADAMS
Department of Chemistry, University of Antwerp (UIA), B-2610 Wilrijk, Belgium

(Received: 4 June 1984)

Abstract. Using laser microprobe mass analysis (LAMMA), it is possible to characterize the inorganic composition of clays and to study adsorption phenomena. Natural sepiolite, loughlinite (Na-sepiolite), montmorillonite and saponite samples from Anatolia (Turkey) have been investigated All the clays gave different fingerprint mass spectra which allowed a quick estimation of the relative amounts of exchangeable cations as well as the trace contaminants and the homogeneity of their distribution. The adsorption behaviour of these clays for pyridine was also studied and it appeared that pyridine molecules penetrated the inner layers, as well as being adsorbed on the external surface.

Key words: adsorption, laser microprobe mass analysis (LAMMA), clay.

1. Introduction

Laser microprobe mass analysis (LAMMA) has high sensitivity and the ability to analyse a wide range of elements [1]. LAMMA also has applications in the study of organic and organometallic compounds [2]. Moreover, adsorption phenomena can be analysed by this method [3]. All these properties make the method attractive for soil research.

Natural clays often contain different impurities and these may affect the adsorption capacity and the reactivity. The adsorption properties of clay minerals, belonging to the montmorillonite-saponite group (smectite) [4], have been studied by several authors using mainly infrared spectroscopy [5–10]. Sepiolite and loughlinite (Na-sepiolite) which have fibrous structures consisting of talc-like ribbons parallel to the fibre axis [11, 12], also have high adsorptive capacity for many gases and vapors [10, 13–17].

★ Author for correspondence.

In this study we analysed the inorganic composition of natural sepiolite, loughlinite, montmorillonite and saponite from Anatolia (Turkey) and examined their adsorption behaviour for pyridine, using LAMMA. The aim of this work is to compare the adsorption capacity of the clays studied and to investigate the penetration profile of the adsorbed molecules.

2. Experimental

Sepiolite and loughlinite samples were obtained from the Mihalliccık region of Eskişehir-Turkey. Montmorillonite and saponite samples were obtained from Küçükhacıbey-Çankırı and Sivas, respectively. The samples were first investigated by X-ray diffraction, *differential* thermal analysis and elemental analysis. In loughlinite, analcime and dolomite were detected as significant impurities. Chemical analyses of the samples were carried out on a GE SPG-7 X-ray fluorescence spectrometer, Jarrell Ash optical emission spectrography or for some elements, using conventional wet analytical methods. The results are summarized in Table I.

Table I. Chemical analysis of the clays (weight %)

Sample	Sepiolite	Loughlinite	Montmorillonite	Saponite
SiO_2	58.0	56.0	58.0	52.0
MgO	25.5	14.0	2.5	10.9
Al_2O_3	0.5	5.3	17.0	13.6
K_2O	0.5	1.0	0.6	2.2
CaO	0.5	1.1	1.0	1.3
$\Sigma(FeO + Fe_2O_3)$	0.05	1.5	5.0	3.5
TiO_2	0.05	0.25	0.6	0.5
Na_2O	0.05	5.9	1.1	n.d.[a]
MnO	n.d.	0.05	0.01	0.02
P_2O_5	n.d.	0.15	0.07	0.03
Ni	0.1	n.d.	0.01	0.02
Cu	n.d.	n.d.	0.002	0.001
LOI[b]	14.5	15.0	14.2	16.0
Total	99.75	100.25	100.09	100.07

[a] Not detected. [b] Loss on ignition.

Pyridine treated samples were prepared by stirring them in liquid pyridine (99 + %, spectrophotometric grade, gold label, Janssen Chimica, Belgium) at room temperature for two days.

The commercially available laser microprobe mass analyser (LAMMA) (LAMMA 500, Leybold-Heraeus, Cologne, FRG) is described in detail in the literature [18–21].

The IR spectra of self supporting thin films of montmorillonite were recorded on a Perkin-Elmer 621 spectrometer.

3. Results and Discussion

3.1. LAMMA SPECTRA OF UNTREATED CLAYS

The positive and negative mass spectra of the clays are characterized by several elemental ion peaks and also by considerable molecular fragment ions which provide significant morphological information concerning structurally lattice bound ions and impurities. All the samples gave different fingerprint mass spectra which allowed the estimation of the relative amounts of exchangeable cations.

Figure 1 shows representative positive and negative LAMMA spectra of untreated sepiolite and loughlinite. The most prominent difference between these samples is the intensity of the Na^+ peak relative to Mg^+ in the positive spectra. Also small differences in the Li^+, Al^+, Ti^+ and Fe^+ intensities can be observed which are due to their inhomogeneous distribution among the individual clay particles.

Although the negative mass spectra of both sepiolites appear to be similar, loughlinite shows more intense AlO^- ($m/e = 43$) and AlO_2^- ($m/e = 59$) molecular ion peaks, in agreement with the chemical composition. Both clays probably have some organic trace contaminants which can be observed from the low intensity peaks of C_2^- ($m/e = 24$), C_2H^- ($m/e = 25$) and $C_2H_2^-$ or CN^- ($m/e = 26$).

Figure 2(a–h) illustrates typical examples of negative mass spectra of untreated sepiolite and loughlinite when four consecutive laser shots of comparable and low laser energy ($\sim 0.4\ \mu J$) are directed at the same location of an individual clay particle. While the SiO_2^- and SiO_3^- peaks are the only important features of the spectra on the first shot (Figure 2 (a) and (e)), on subsequent laser shots, one notes the contribution of H^-, O^- and OH^- ions due to the bound water or structural OH-groups, $[MgO \cdot SiO_2]^-$ and $[MgO \cdot H(SiO_3)]^-$ ions due to the magnesium—silicon bonds through oxygen bridges, and finally the main Si_2O_5 units of the sepiolite structure, from the inner sample layers.

The positive and negative LAMMA spectra of montmorillonite and saponite follow the same general characteristics. Both clays contain iron and titanium cations, inhomogeneously distributed among the particles.

3.2. LAMMA SPECTRA OF PYRIDINE-TREATED CLAYS

3.2.1. *Sepiolites*

We did not observe the pyridine molecular ion peak at $m/e = 79$ in any positive mass spectrum of the samples studied. Only three positive spectra of the pyridine treated sepiolite, out of a total of 14, showed a low intensity protonated pyridine peak at $m/e = 80$, and none of the positive spectra of the pyridine-treated loughlinite gave a peak at $m/e = 80$. However, every negative spectrum of pyridine-treated clays showed a prominent fragmentation peak of pyridine derived CN^- at $m/e = 26$ (Figure 3) which was absent or lower in intensity by at least one order of magnitude in the spectra of untreated clays (Figure 2). Since we did not observe any pyridinium band in the infrared spectrum of pyridine-treated sepiolite [16], this protonated species most likely originated from adsorbed pyridine through the laser ionization process.

Figure 3(a–h) shows typical examples of negative mass spectra of pyridine treated sepiolite and loughlinite following consecutive laser shots of $0.4\ \mu J$ on the same location of a clay particle. The prominent molecular fragment ion (CN^-) of the pyridine molecule at $m/e = 26$ is observed at the inner layers of the treated sample as well as at the surface. In comparing the LAMMA spectra of sepiolite with those of loughlinite it appears that sepiolite adsorbs the product somewhat more strongly.

Although the molecular fragment, (CN^-), of the pyridine molecule is observed in all the negative spectra of the treated sepiolites as the most intense peak, it is no longer observed after refluxing pyridine-treated samples in water for 24 h which is in agreement with infrared spectroscopic results [16].

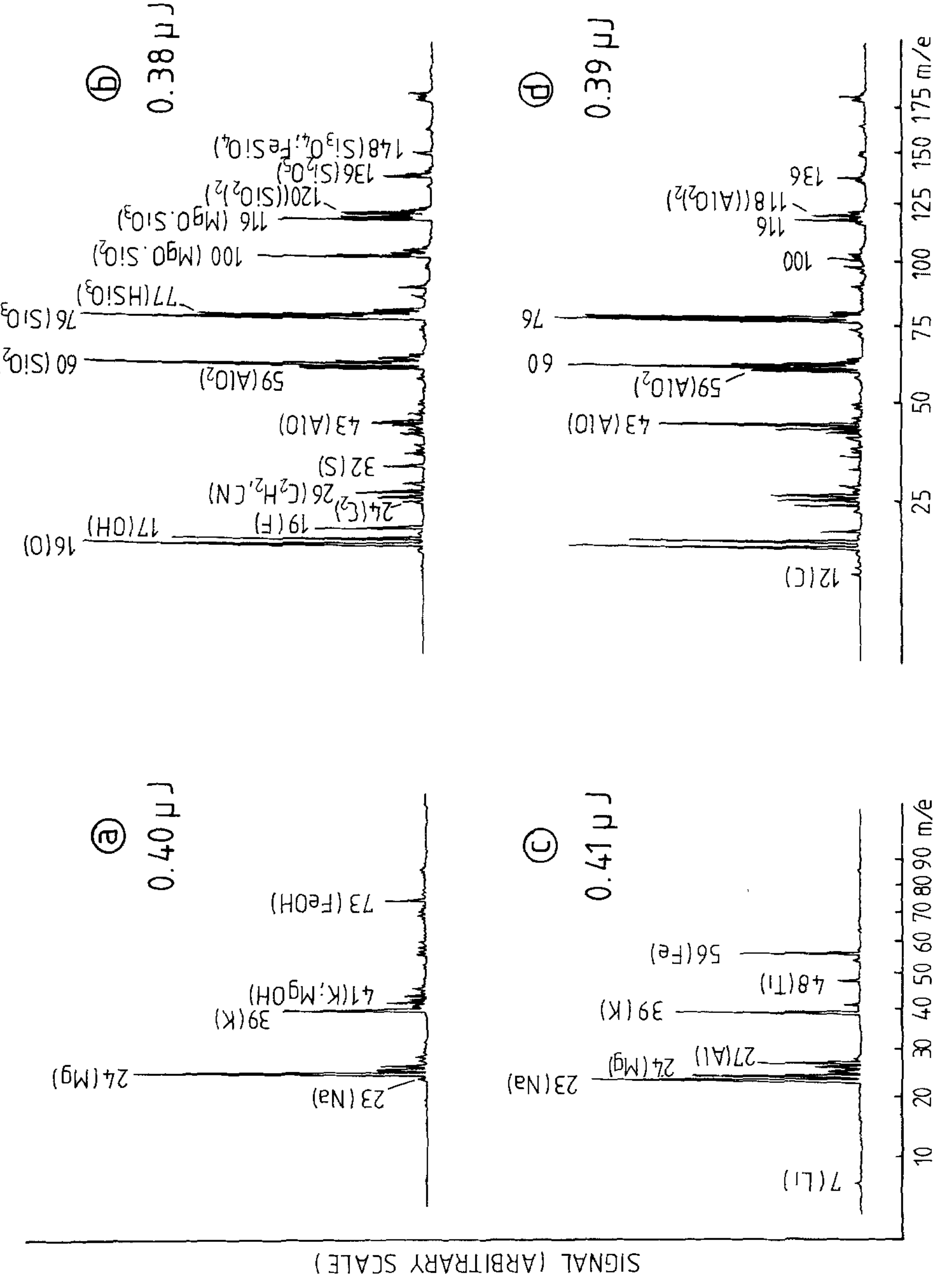

Fig. 1. Positive (a, c) and negative (b, d) LAMMA spectra of sepiolite (a, b) and loughlinite (c, d).

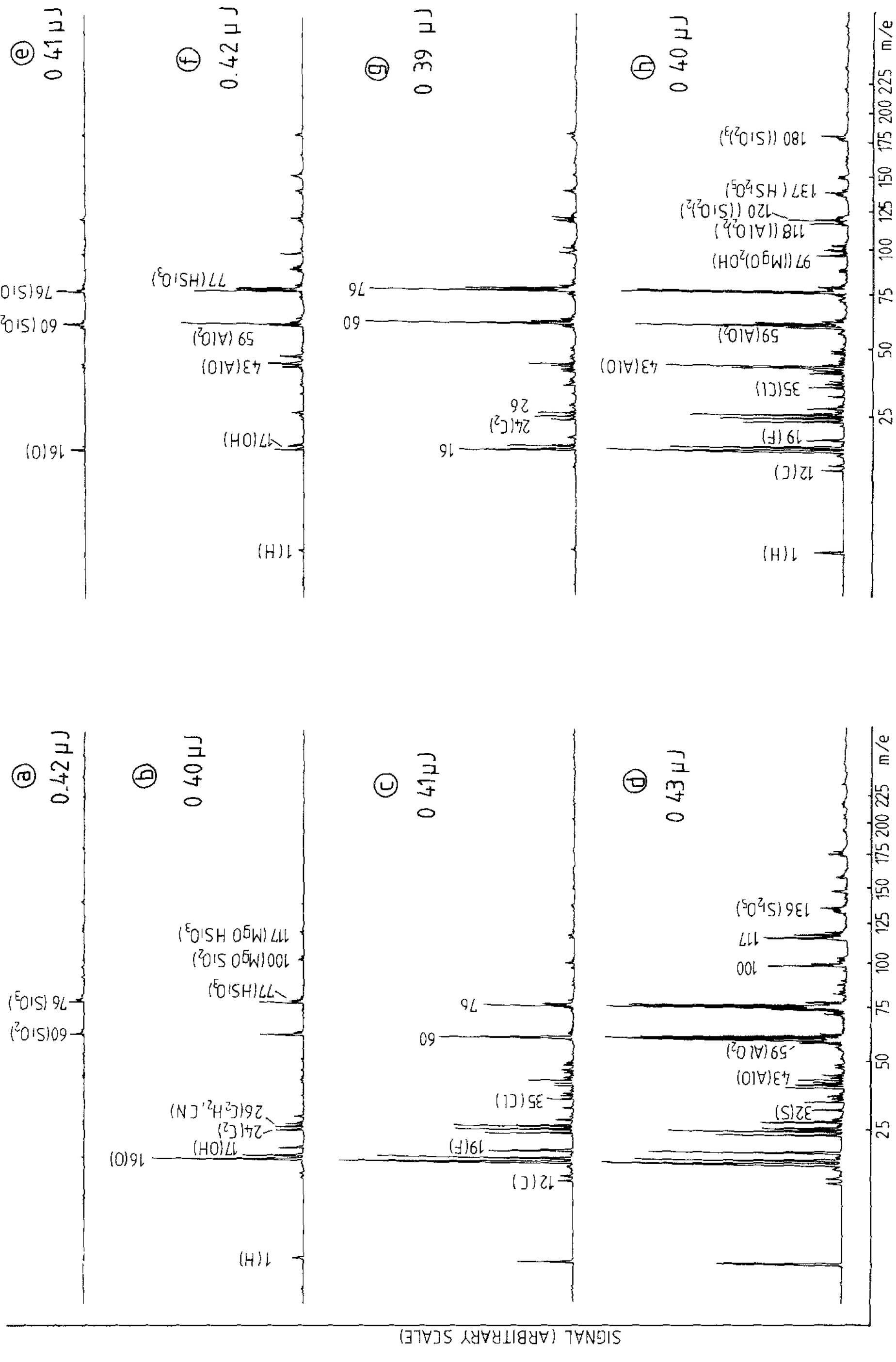

Fig. 2. Negative LAMMA spectra of sepiolite (a–d) and loughlinite (e–h) with four consecutive laser shots (~0.4 μJ).

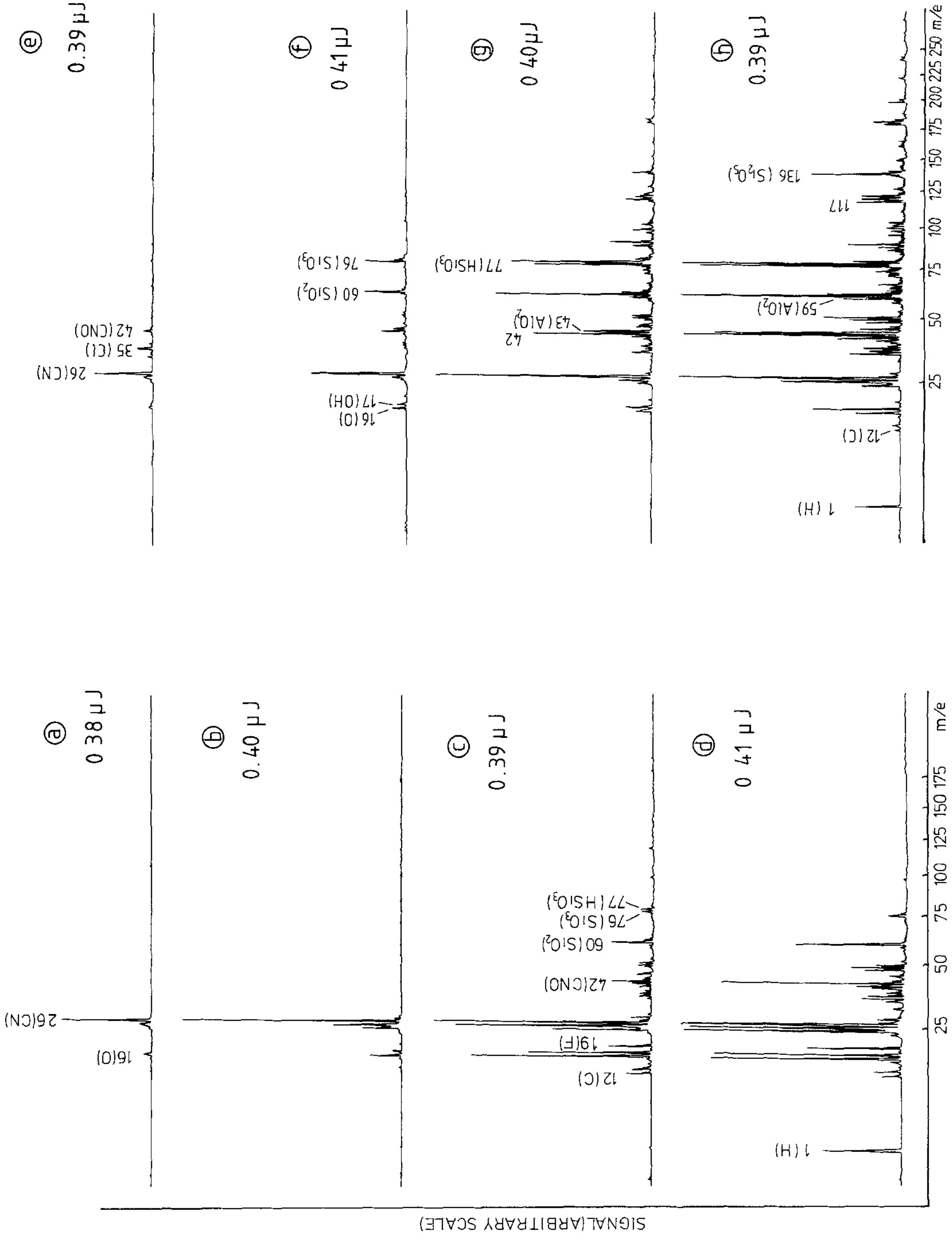

Fig. 3. Negative LAMMA spectra of pyridine-treated sepiolite (a–d) and loughlinite (e–h) with four consecutive laser shots (~0.4 μJ).

3.2.2. *Saponite*

Although we did not observe either a pyridine ($m/e = 79$) or a protonated pyridine ($m/e = 80$) molecular ion peak, the fragmentation peak of pyridine (CN^-) is again observed as the most intense feature in all the negative spectra.

3.2.3. *Montmorillonite*

Positive LAMMA spectra of pyridine-treated montmorillonite showed different phenomena from those of the other treated clays. Almost every positive spectrum showed a protonated pyridine peak at $m/e = 80$ and moreover, cluster ions of pyridine [$(2C_5H_5N{-}H)^+$, $(3C_5H_5N{-}H)^+$] were also observed (Figure 4). These peaks completely disappear after refluxing the treated sample in water for three days. Since it is known that, depending on the nature of the exchangeable cation, pyridinium ion can be formed from the adsorption of pyridine by montmorillonite [5], to shed light on the protonated pyridine peak ($m/e = 80$) in the positive LAMMA spectrum we also recorded the IR spectrum of this sample. The IR spectrum showed all the characteristics of the coordinated pyridine [5], but we did not observe any pyridinium band [5,22]. Thus this protonated pyridine molecular ion was most likely formed by a laser ionization process.

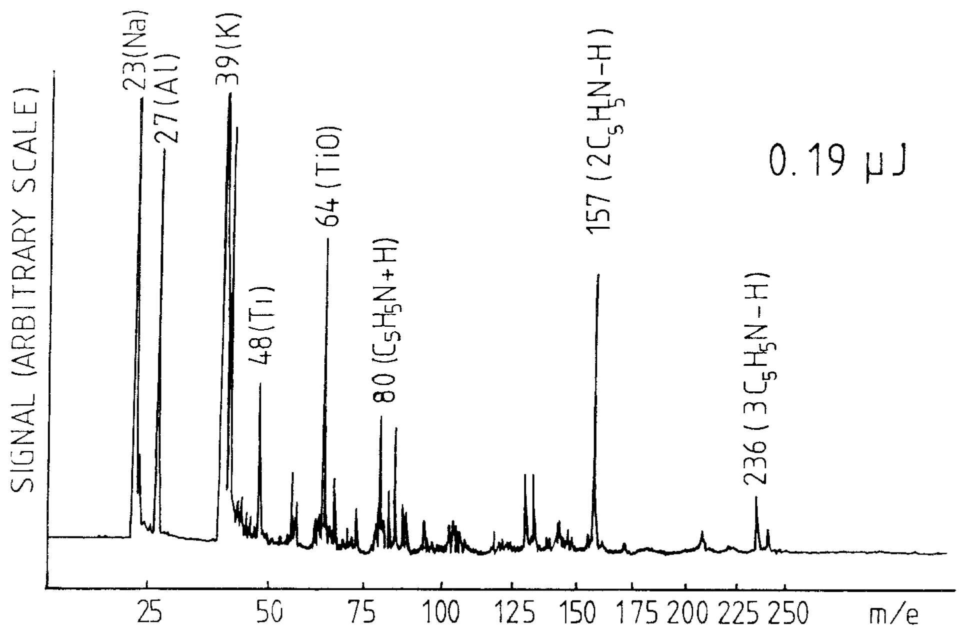

Fig.4. Positive LAMMA spectrum of pyridine-treated montmorillonite.

Negative LAMMA spectra of pyridine-treated montmorillonite showed the same characteristics as those of saponite and sepiolites with the fragmentation peak of pyridine at $m/e = 26$ (CN^-) as the prominent feature.

The pyridine treated sample acquired a pale blue colour. This colour change was previously observed on adsorption of pyridine on Na- and Mg-montmorillonite [5, 23] after longer treatment (by keeping the sample in liquid pyridine for 14 days [5]), and was ascribed to the formation of a pyridine free radical. Farmer and Mortland [5] postulated that this was due to the catalytic action of copper ions. In our samples the copper content is too low to support this hypothesis. On the other hand, in contrast to Barrer and Macleod [23], we found that the coloration with pyridine is a reversible process. We obtained exactly the same positive and negative LAMMA spectra corresponding to those of untreated clay after refluxing the treated sample in water.

4. Conclusions

LAMMA allows a very quick analysis of inorganic and organic contents of clays, particularly as it gives a rough idea about the relative amounts of exchangeable cations and the homogeneity of their distribution. This knowledge is important in catalysis and adsorption studies, since the catalytic and sorptive properties of clays are known to depend strongly on the nature of exchangeable cations in the structure [24–26].

The adsorption and reactive properties of the montmorillonite sample is markedly different from that of other clay minerals with prominent cluster peaks, $[(2C_5H_5N{-}H)^+$, $(3C_5H_5N{-}H)^+]$. Similar peaks were previously observed in the positive LAMMA spectra of organometallic compounds [2]. On the other hand, although we do not observe any unusual IR absorption of pyridine except for the coordinated pyridine characteristics, the coloration of montmorillonite with pyridine is still an open question. An ESR study would be necessary to solve this problem. We are presently working on it and the results will be published elsewhere.

Acknowledgements

This research was funded by the EEC through research grant No. ENV-620-B(RS) and by the Interministrial Commission for Science Policy, Belgium, through research grant 80-85/10. J.D.W. is indebted to the Instituut tot Aanmoediging van het Wetenschappelijk Onderzoek in Nijverheid en Landbouw (IWONL) for financial support.

References

1. S. Henstra, E. B. Bisdom, A. Jongerius, H. J. Heinen, and S. Heier: *Z. Anal. Chem.* **308**, 280 (1981).
2. J. F. Muller, C. Berthé, and J. M. Magar: *Z. Anal. Chem.* **308**, 312 (1981).
3. J. K. De Waele, I. Verhaert, E. F. Vansant, and F. C. Adams: *Surface and Interface Anal.* **5**, 186 (1983).
4. B. K. G. Theng: *The Chemistry of Clay-Organic Reactions*, p. 9, John Wiley (1974).
5. V. C. Farmer and M. M. Mortland: *J. Chem. Soc. (A)* 344 (1966).
6. J. M. Serratosa: *Clays Clay Min.* **14**, 385 (1966).
7. R. L. Parfitt and M. M. Mortland: *Soil Sci. Soc. Am. Proc.* **32**, 355 (1968).
8. P. Cloos, A. Moreale, C. Broers, and C. Badot: *Clay Min.* **14**, 307 (1979).
9. V. Lorprayoon and R. A. Condrate: *Appl. Spectrosc.* **36**, 696 (1982).
10. R. M. Barrer, N. Mackenzie, and D. M. Macleod: *J. Phys. Chem.* **58**, 568 (1954).
11. K. Brauner and A. Preisinger: *Tschermaks Min. Petr. Mitt.* **6**, 120 (1956).
12. J. J. Fahey, M. Ross, and J. M. Axelrod: *Am. Min.* **45**, 270 (1960).
13. A. J. Dandy: *J. Phys. Chem.* **72**, 334 (1968).
14. A. J. Dandy: *J. Chem. Soc.* 2383 (1971).
15. C. Serna and T. Fernandez-Alvarez: *An. Quim.* **71**, 371 (1975).
16. S. Akyüz and T. Akyüz: *Hacettepe Bull. Natural Sci. Eng.* **11**, 47 (1982).

17. S. Akyüz and T. Akyüz: *Hacettepe Bull. Natural Sci. Eng.* **12**, 157 (1983).
18. H. Vogt, H. J. Heinen, S. Meier, and R. Wechsung: *Z. Anal. Chem.* **308**, 195 (1981).
19. R. Kaufmann, H. Hillenkamp and R. Wechsung: *Med. Progr. Technol.* **6**, 109 (1979).
20. E. Denoyer, R. Van Grieken, F. C. Adams and D. F. S. Natusch: *Anal. Chem.* **54**, 26A (1982).
21. D. M. Hercules, R. J. Day, K. Balasonmugan, T. A. Dand, and C. P. Li: *Anal. Chem.* **54**, 280A (1982).
22. J. M. Serratosa: *Clays Clay Min.* **16**, 93 (1968).
23. R. M. Barrer and D. M. Macleod: *Trans. Faraday Soc.* **50**, 980 (1954).
24. F. Annabi-Bergaya, M. I. Cruz, L. Gatineau, and J. J. Fripiat: *Clay Min.* **16**, 115 (1981).
25. R. Keren and G. A. O'Connor: *Clays Clay Min.* **30**, 341 (1982).
26. Y. Kiyatama and A. Michishita: *J. Chem. Soc. Chem. Commun.* 401 (1981).